

NASA Technical Memorandum 100554

**AN ANALYTICAL STUDY OF THE EFFECTS OF TRANSVERSE
SHEAR DEFORMATION AND ANISOTROPY ON NATURAL VIBRATION
FREQUENCIES OF LAMINATED CYLINDERS**

**(NASA-TM-100554) AN ANALYTICAL STUDY OF THE
EFFECTS OF TRANSVERSE SHEAR DEFORMATION AND
ANISOTROPY ON NATURAL VIBRATION FREQUENCIES
OF LAMINATED CYLINDERS (NASA) 36 pCSCL 11D**

N88-17739

Unclas

G3/24 0124960

DAWN C. JEGLEY

JANUARY 1988

NASA

**National Aeronautics and
Space Administration**

**Langley Research Center
Hampton, Virginia 23665**

ABSTRACT

Natural vibration frequencies of orthotropic and anisotropic simply supported right circular cylinders are predicted using a higher-order transverse-shear deformation theory. A comparison of natural vibration frequencies predicted by first-order transverse-shear deformation theory and the higher-order theory shows that an additional allowance for transverse shear deformation has a negligible effect on the lowest predicted natural vibration frequencies of laminated cylinders but significantly reduces the higher natural vibration frequencies. A parametric study of the effects of ply orientation on the natural vibration frequencies of laminated cylinders indicates that while stacking sequence affects natural vibration frequencies, cylinder geometry is more important in accurately predicting transverse-shear deformation effects. Interaction curves for cylinders subjected to axial compressive loadings and low natural vibration frequencies indicate that transverse shearing effects are less important in predicting low natural vibration frequencies than in predicting axial compressive buckling loads. The effects of anisotropy are more important than the effects of transverse shear deformation for most strongly anisotropic laminated cylinders in predicting natural vibration frequencies. However, transverse-shear deformation effects are important in predicting high natural vibration frequencies of thick-walled laminated cylinders. Neglecting either anisotropic effects or transverse-shear deformation effects leads to non-conservative errors in predicted natural vibration frequencies.

INTRODUCTION

Laminated composite materials have high strength-to-weight and stiffness-to-weight ratios that make them useful for building light-weight structural components. However, composite materials also have low transverse shear moduli which permit more transverse shearing to occur in composites than in metals. As a result, composite cylinders can have lower natural vibration frequencies than predicted by conventional first-order transverse-shear-deformation shell theory. Since laminated composites are increasingly being used as structural components, the effects of transverse shear deformation should be taken into account in designing laminated components to assure that the natural vibration frequencies of these structures are evaluated accurately. An extensive survey of shell vibration work up to 1973 is presented in reference 1. In reference 1, transverse shear deformation and orthotropy are discussed but anisotropy is only briefly mentioned. Some work has been done in the area of vibration of composite cylinders (e.g., ref. 2-5), but few studies account for both transverse shear deformation and anisotropic effects.

For laminated cylinders, the effects of transverse shear deformation on low natural vibration frequencies with long wavelengths are small and conventional first-order transverse-shear deformation theory accurately predicts the lowest frequencies. For higher frequencies with short wavelengths, transverse-shear deformation effects can become important and predictions based on the first-order theory are not always accurate. First-order transverse-shear deformation theory takes into account some of the effects of transverse shearing and predicts accurate natural vibration frequencies for low frequencies, but this theory is insufficient to account

for the amount of transverse shearing in some thick-walled laminated cylinders vibrating at high frequencies.

Predictions of natural vibration frequencies are found by using a procedure similar to that used to find critical buckling loads. In the theory developed in references 6 and 7 for predicting buckling loads of shells, the three-dimensional equations of elasticity are reduced to two dimensions by assuming trigonometric functions in the thickness direction for strains and displacements in addition to the constant and linear terms more commonly used. The assumed displacements and stresses can be reduced to those of the first-order transverse-shear deformation shell theory by removing the through-the-thickness trigonometric terms. A variational procedure is applied to the equations of elasticity to obtain differential equations using the potential energy method. Nine assumed displacement terms are used in reference 6 so the variational procedure yields nine simultaneous second-order differential equations. These resulting differential equations are left in terms of integrals in the axial and radial directions and are functions of stresses and derivatives of stresses. These differential equations are solved to find numerical values of buckling loads in reference 8.

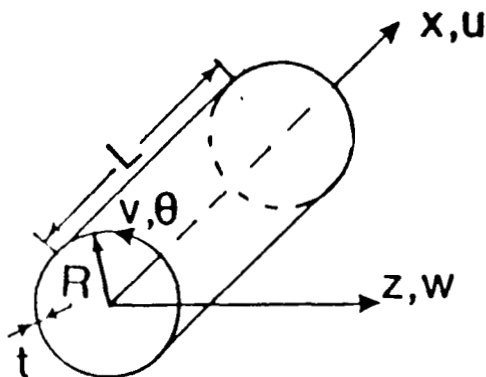
In the present paper the natural vibration frequencies of orthotropic and anisotropic simply supported right circular cylinders are predicted using a theory which takes into account higher-order transverse-shear deformation effects. The equilibrium equations presented in reference 8 are solved to find natural vibration frequencies instead of critical buckling loads. The eigenvalue problem is solved numerically to obtain the natural vibration frequencies of several types of cylinders. A comparison is made

between results based on first-order transverse-shear deformation theory and the higher-order theory.

Ply orientation can affect the reduction in natural vibration frequencies due to transverse shear deformation. Results of a parametric study of ply orientations for two classes of laminates, $[\pm\theta/90]_{4s}$ and $[\pm\theta]_s$, are presented for values of θ ranging from 0° to 90° . The interaction of critical axial compressive loads and natural vibration frequencies for laminated cylinders of orthotropic and anisotropic stacking sequences is also presented.

ANALYSIS APPROACH

The results presented in this paper are obtained by applying the theory presented in references 6-8. In these references the potential energy method is used to obtain equations for the buckling of right circular cylinders using a coordinate system with axes (x, θ, z) , displacements (u, v, w) , and cylinder dimensions (L, R, t) as shown in the sketch.



Vibration of Orthotropic Cylinders

The cylinder displacements assumed in this study to represent the higher-order thickness effects of transverse shear deformation in orthotropic cylinders are shown in equations (1).

$$\begin{aligned}u &= u^o + u^a (z/t) + u^1 \sin(\pi z/t) \\v &= v^o + v^a (z/t) + v^1 \sin(\pi z/t) \\w &= w^o + w^a (z/t) + w^1 \cos(\pi z/t)\end{aligned}\tag{1}$$

The series in equations (1) have three types of terms, all of which are functions of x and θ . The traditional terms from classical Kirchhoff-Love theory (those independent of position in the radial direction) are represented by superscript o . The displacements of classical Kirchhoff-Love theory can be obtained by neglecting the superscript 1 terms and the w^a term and by assuming that $u^a = -w^o_{,x}$ and that $v^a = -w^o_{,y}$ in equations (1). The additional terms associated with conventional Reissner-Mindlin first-order transverse-shear deformation theory (those linear in z) are represented by superscript a . The displacements of conventional Reissner-Mindlin first-order transverse-shear deformation theory can be obtained by neglecting the superscript 1 and the w^a terms. The assumed displacement series also includes trigonometric terms in the through-the-thickness (radial) direction, which are represented by the terms with superscript 1. By including these additional terms in the assumed displacement series, a more accurate solution can be obtained because more three-dimensional

effects are permitted than in the solutions with fewer assumed displacement terms.

Differential equations and boundary conditions for predicting the buckling loads of right circular cylinders are developed in reference 8 by using the potential energy method. The method used in reference 8 for predicting buckling loads is used in this paper to predict natural vibration frequencies. The virtual work of the cylinder is shown in equation (2).

$$\delta \Pi = \int_{\text{Vol}} (\sigma_x \delta \epsilon_x + \sigma_\theta \delta \epsilon_\theta + \sigma_z \delta \epsilon_z + \tau_{x\theta} \delta \gamma_{x\theta} + \tau_{xz} \delta \gamma_{xz} + \tau_{z\theta} \delta \gamma_{z\theta} - \rho \omega^2 (u \delta u + v \delta v + w \delta w)) d \text{Vol} \quad (2)$$

where σ_x , σ_θ , σ_z , $\tau_{x\theta}$, τ_{xz} , and $\tau_{z\theta}$ are the stresses, ϵ_x , ϵ_θ , ϵ_z , $\gamma_{x\theta}$, γ_{xz} , and $\gamma_{z\theta}$ are the strains, ρ is the density, and ω is the natural vibration frequency of the cylinder.

The differential equations used to derive equilibrium equations based on the displacements in equations (1) are presented in references 6-8. The differential equations in references 6-8, modified to account for vibration frequencies instead of compressive buckling loads, are presented in equations (3). Since there are nine assumed displacement terms, there are nine differential equations.

$$\int_{-t/2}^{t/2} [\sigma_{x,x} + \frac{\tau_{x\theta,x}}{R} - \rho L \omega^2 / 2 u] \delta u^0 dz = 0$$

$$\int_{-t/2}^{t/2} [\frac{\sigma_{\theta,\theta}}{R} + \tau_{x\theta,x} + \frac{\tau_{\theta z}}{R} - \rho L \omega^2 / 2 v] \delta v^0 dz = 0$$

$$\begin{aligned}
& \int_{-t/2}^{t/2} \left[-\frac{\sigma_{\theta}}{R} + \tau_{xz',x} + \frac{\tau_{\theta z',\theta}}{R} - \rho L \omega^2 / 2 w \right] \delta w^0 dz = 0 \\
& \int_{-t/2}^{t/2} \left[\left(\sigma_{x',x} + \frac{\tau_{x\theta',\theta}}{R} \right) \frac{z}{t} - \frac{\tau_{xz}}{t} - \rho L \omega^2 / 2 u \frac{z}{t} \right] \delta u^a dz = 0 \\
& \int_{-t/2}^{t/2} \left[\left(\frac{\sigma_{\theta',\theta}}{R} + \tau_{x\theta',x} \right) \frac{z}{t} - \frac{\tau_{\theta z}}{t} + \frac{\tau_{\theta z}}{R} \frac{z}{t} - \rho L \omega^2 / 2 v \frac{z}{t} \right] \delta v^a dz = 0 \quad (3) \\
& \int_{-t/2}^{t/2} \left[\left(-\frac{\sigma_{\theta}}{R} + \tau_{xz',x} + \frac{\tau_{\theta z',\theta}}{R} \right) \frac{z}{t} + \frac{\sigma_z}{t} - \rho L \omega^2 / 2 w \frac{z}{t} \right] \delta w^a dz = 0 \\
& \int_{-t/2}^{t/2} \left[\left(\sigma_{x',x} + \frac{\tau_{x\theta',\theta}}{R} \right) \sin \left(\frac{\pi z}{t} \right) - \tau_{xz} \frac{\pi}{t} \cos \left(\frac{\pi z}{t} \right) - \right. \\
& \qquad \qquad \qquad \left. \rho L \omega^2 / 2 u \sin \left(\frac{\pi z}{t} \right) \right] \delta u^1 dz = 0 \\
& \int_{-t/2}^{t/2} \left[\left(\frac{\sigma_{\theta',\theta}}{R} + \tau_{x\theta',x} \right) \sin \left(\frac{\pi z}{t} \right) - \frac{\pi}{t} \tau_{\theta z} \cos \left(\frac{\pi z}{t} \right) + \frac{\tau_{\theta z}}{R} \sin \left(\frac{\pi z}{t} \right) \right. \\
& \qquad \qquad \qquad \left. - \rho L \omega^2 / 2 v \sin \left(\frac{\pi z}{t} \right) \right] \delta v^1 dz = 0 \\
& \int_{-t/2}^{t/2} \left[\left(-\frac{\sigma_{\theta}}{R} + \tau_{xz',x} + \frac{\tau_{\theta z',\theta}}{R} \right) \cos \left(\frac{\pi z}{t} \right) + \frac{\pi}{t} \sigma_z \sin \left(\frac{\pi z}{t} \right) \right. \\
& \qquad \qquad \qquad \left. - \rho L \omega^2 / 2 w \cos \left(\frac{\pi z}{t} \right) \right] \delta w^1 dz = 0
\end{aligned}$$

where δu^0 , δu^a , δu^1 , ... are the displacement variations. The equilibrium equations for the cylinder are obtained from equations (3) by integrating by parts.

The differential equations represented by the arguments of equations (3) can be reduced to linear equations containing only the displacements and natural vibration frequencies as unknowns by using the following stress-strain and strain-displacement relations as derived in references 6 and 9 (and neglecting all nonlinear terms).

$$\begin{aligned}
\{\sigma\} &= [C_{ij}] \{\epsilon\} \\
\epsilon_x &= u_{,x} \\
\epsilon_\theta &= \frac{1}{R}(w + v_{,\theta}) \\
\epsilon_z &= \frac{\bar{w}^a}{t} - w^1 \frac{\pi}{t} \sin\left(\frac{\pi z}{t}\right) \\
\gamma_{x\theta} &= \frac{u_{,\theta}}{R} + v_{,x} \\
\gamma_{xz} &= \frac{u^a}{t} + \frac{\pi}{t} u^1 \cos\left(\frac{\pi z}{t}\right) + w_{,x} \\
\gamma_{\theta z} &= \frac{v^a}{t} + \frac{\pi}{t} v^1 \cos\left(\frac{\pi z}{t}\right) + \frac{1}{R}(w_{,\theta} - v)
\end{aligned} \tag{4}$$

where $[C_{ij}]$ is the orthotropic material stiffness matrix.

The dependence of the displacements on the axial and circumferential coordinates can be expressed in the form:

$$\begin{aligned}
u &= [\bar{u}^0 + \bar{u}^a(z/t) + \bar{u}^1 \sin(\pi z/t)] \cos(m\pi x/L) \sin(n\theta) \\
v &= [\bar{v}^0 + \bar{v}^a(z/t) + \bar{v}^1 \sin(\pi z/t)] \sin(m\pi x/L) \cos(n\theta) \\
w &= [\bar{w}^0 + \bar{w}^a(z/t) + \bar{w}^1 \cos(\pi z/t)] \sin(m\pi x/L) \sin(n\theta)
\end{aligned} \tag{5}$$

where the superscripted terms are constants (independent of position). The cylinder displacement pattern is assumed to consist of m half waves in the longitudinal direction and n full waves in the circumferential direction. Simple support boundary conditions $w = w_{,xx} = v = u_{,x} = 0$ are assumed.

Substituting equations (4) and (5) into equations (3) and integrating in the radial direction gives the following equations:

$$\alpha \bar{u}^0 + \beta \bar{v}^0 + \psi \bar{w}^0 + \frac{2}{\pi} \psi \bar{w}^1 = \rho L \omega^2 / 2 u^0$$

$$\beta \bar{u}^0 + \Delta \bar{v}^0 + \kappa \bar{w}^0 - \xi \bar{v}^a + 2\xi \bar{v}^1 + \frac{2}{\pi} \kappa \bar{w}^1 = \rho L \omega^2 / 2 v^0$$

$$\begin{aligned} \psi \bar{u}^0 + \kappa \bar{v}^0 + \eta \bar{w}^0 + G_{xz} \frac{m\pi}{L} \bar{u}^a + \xi n \bar{v}^a + G_{xz} \frac{2m\pi}{L} \bar{u}^1 + 2n\xi \bar{v}^1 + \frac{2}{\pi} \eta \bar{w}^1 \\ = \rho L \omega^2 / 2 (w^0 + w^1 \frac{2}{\pi}) \end{aligned}$$

$$\begin{aligned} G_{xz} \frac{m\pi}{L} \bar{w}^0 + (\frac{\alpha}{12} + \frac{G_{xz}}{t}) \bar{u}^a + \frac{\beta}{12} \bar{v}^a + \frac{\psi}{12} \bar{w}^a + (\frac{\alpha}{\pi^2} + G_{xz} \frac{2}{t}) \bar{u}^1 \\ + \frac{\beta}{\pi^2} \bar{v}^1 + G_{xz} \frac{2m}{L} \bar{w}^1 = \rho L \omega^2 / 2 (\frac{u^a}{12} + 2\frac{u^1}{\pi^2}) \end{aligned}$$

$$\begin{aligned} -\xi \bar{v}^0 + \xi n \bar{w}^0 + \frac{\beta}{12} \bar{u}^a + [\Delta/12 + G_{z\theta}/t] \bar{v}^a + \frac{\kappa}{12} \bar{w}^a + \beta \bar{u}^1 + \\ [\Delta/\pi^2 + \frac{2}{t} G_{z\theta}] \bar{v}^1 + \xi \frac{2n-1}{\pi} \bar{w}^1 = \rho L \omega^2 / 2 (\frac{v^a}{12} + 2\frac{v^1}{\pi^2}) \end{aligned}$$

$$\psi/12 \bar{u}^a + \frac{\kappa}{12} \bar{v}^a + (\frac{\eta}{12} + \frac{Q_{33}}{t}) \bar{w}^a + \frac{\psi}{\pi^2} \bar{u}^1 + \frac{\kappa}{\pi^2} \bar{v}^1 = \rho L \omega^2 / 2 w^a / 12 \quad (6)$$

$$\begin{aligned} G_{xz} \frac{2m\pi}{L} \bar{w}^0 + (\frac{\alpha}{\pi^2} + G_{xz} (\frac{2\pi}{t})) \bar{u}^a + \beta/\pi^2 \bar{v}^a + \frac{\psi}{\pi^2} \bar{w}^a + \frac{1}{2} (\alpha + G_{xz} \frac{\pi^2}{t}) \bar{u}^1 \\ + \frac{1}{2} \beta \bar{v}^1 + G_{xz} \frac{m\pi^2}{2L} \bar{w}^0 = \rho L \omega^2 / 2 (2\frac{u^a}{\pi^2} + \frac{u^1}{2}) \end{aligned}$$

$$\begin{aligned} -\xi \frac{2}{\pi} \bar{v}^0 + \xi 2n \bar{w}^0 + \beta/\pi^2 \bar{u}^a + [\Delta/\pi^2 + \frac{2}{t} G_{z\theta}] \bar{v}^a + \frac{\kappa}{\pi^2} \bar{w}^a + \frac{\beta}{2} \bar{u}^1 + \\ [\Delta + \frac{\pi^2}{t} G_{z\theta}] \bar{v}^1 + \frac{n\pi}{2} \xi \bar{w}^1 = \rho L \omega^2 / 2 (2\frac{v^a}{\pi^2} + \frac{v^1}{2}) \end{aligned}$$

$$\begin{aligned} \frac{2}{\pi} \xi \bar{u}^0 + \frac{2}{\pi} \kappa \bar{v}^0 + \frac{2}{\pi} \eta \bar{w}^0 + G_{xz} \frac{2m}{L} \bar{u}^a + \xi \frac{2n}{\pi} \bar{v}^a + G_{xz} \frac{m\pi^2}{2L} \bar{u}^1 + \frac{n\pi}{2} \xi \bar{v}^1 + \\ (\eta + \frac{\pi^2}{t} C_{33}) \frac{1}{2} \bar{w}^1 = \rho L \omega^2 / 2 (2\frac{w^0}{\pi} + \frac{w^1}{2}) \end{aligned}$$

where $\alpha = [C_{11} (m\pi/L)^2 + G_{x\theta} (n/R)^2] t$

$\beta = (C_{12} + G_{x\theta}) m n \pi t / (R L)$

$\psi = -C_{12} m t \pi / (R L)$

$$\Delta = [C_{22} (n/R)^2 + G_{x\theta} (m\pi/L)^2 + G_{z\theta}/R^2] t$$

$$\kappa = -(C_{22} + G_{x\theta})(n/R)^2 t$$

$$\eta = [C_{22}/R^2 + G_{xz} (m\pi/L)^2 + G_{z\theta} (n/R)^2] t$$

$$\xi = G_{z\theta}/R$$

and C_{11} , C_{12} , C_{22} , $G_{x\theta}$, G_{xz} , and $G_{\theta x}$ are properties of the cylinder wall.

Natural vibration frequencies can be found by reducing equations (6) to matrix form as shown in equation (7).

$$[K] \begin{Bmatrix} -o \\ \bar{u} \\ -o \\ \bar{v} \\ -o \\ \bar{w} \\ -a \\ \bar{u} \\ -a \\ \bar{v} \\ -a \\ \bar{w} \\ -1 \\ \bar{u} \\ -1 \\ \bar{v} \\ -1 \\ \bar{w} \end{Bmatrix} = \omega^2 [B] \begin{Bmatrix} -o \\ \bar{u} \\ -o \\ \bar{v} \\ -o \\ \bar{w} \\ -a \\ \bar{u} \\ -a \\ \bar{v} \\ -a \\ \bar{w} \\ -1 \\ \bar{u} \\ -1 \\ \bar{v} \\ -1 \\ \bar{w} \end{Bmatrix} \quad (7)$$

The matrix $[K]$ contains the coefficients of the displacement terms on the left hand side of equations (6) and the matrix $[B]$ contains the coefficients of the displacement terms associated with the natural vibration frequency on the right hand side of equations (6). The values of ω^2 which are solutions to the eigenvalue problem in equation (7) are the squares of the natural vibration frequencies.

If the natural vibration frequencies of a cylinder subjected to axial compression are to be found, a value for the applied compressive load must be selected and included in the matrix [K] as discussed in reference 8.

Vibration of Anisotropic Cylinders

The formulation of the eigenvalue problem for anisotropic cylinders is similar to the formulation of the eigenvalue problem for orthotropic cylinders. The same equilibrium and strain-displacement equations are used in the analysis of the anisotropic cylinders as in the analysis of the orthotropic cylinders, as shown in equations (2-4). The stress-strain equations are altered to include the anisotropic effects which are represented by the C_{16} and C_{26} terms in equations (8).

$$\begin{aligned}
 \sigma_x &= C_{11} \epsilon_x + C_{12} \epsilon_\theta + C_{16} \gamma_{x\theta} \\
 \sigma_\theta &= C_{12} \epsilon_x + C_{22} \epsilon_\theta + C_{26} \gamma_{x\theta} \\
 \tau_{x\theta} &= C_{16} \epsilon_x + C_{26} \epsilon_\theta + C_{66} \gamma_{x\theta}
 \end{aligned}
 \tag{8}$$

The displacements used in the anisotropic analysis are similar to those given in equations (5), but the series are expanded to include the sum of several values of m while retaining only one value of n . Several values of m are included to account for displacements in the axial direction which are not in the shape of a pure sine wave. Two Fourier series in the axial direction are used to represent the displacements in the radial direction. One series includes symmetric modes and one series includes antisymmetric modes. Each series is truncated when enough terms have been

included to reach convergence. Similar assumptions are made for the displacement series in the axial and circumferential directions. The assumed displacements for an anisotropic cylinder are given in equations (9) where a total of N terms are included in each displacement.

$$\begin{aligned}
 u &= \sum_{i=1,3,5}^N [\bar{u}_i^0 + \bar{u}_i^a (z/t) + \bar{u}_i^1 \sin(\pi z/t)] \cos(m_i \pi x/L) \sin(n\theta) \\
 &+ \sum_{j=2,4,6}^N [\bar{u}_j^0 + \bar{u}_j^a (z/t) + \bar{u}_j^1 \sin(\pi z/t)] \cos(m_j \pi x/L) \cos(n\theta) \\
 v &= \sum_{i=1,3,5}^N [\bar{v}_i^0 + \bar{v}_i^a (z/t) + \bar{v}_i^1 \sin(\pi z/t)] \sin(m_i \pi x/L) \cos(n\theta) \\
 &+ \sum_{j=2,4,6}^N [\bar{v}_j^0 + \bar{v}_j^a (z/t) + \bar{v}_j^1 \sin(\pi z/t)] \sin(m_j \pi x/L) \sin(n\theta) \quad (9) \\
 w &= \sum_{i=1,3,5}^N [\bar{w}_i^0 + \bar{w}_i^a (z/t) + \bar{w}_i^1 \sin(\pi z/t)] \sin(m_i \pi x/L) \sin(n\theta) \\
 &+ \sum_{j=2,4,6}^N [\bar{w}_j^0 + \bar{w}_j^a (z/t) + \bar{w}_j^1 \sin(\pi z/t)] \sin(m_j \pi x/L) \cos(n\theta)
 \end{aligned}$$

The same procedure for reducing the differential equations of equilibrium to linear equations used for the analysis of the orthotropic cylinders is used for the analysis of the anisotropic cylinders. The same boundary conditions assumed for the orthotropic analysis are assumed for the anisotropic analysis. There are nine equations and nine unknown displacements for each value of m for the displacements represented by equations (9). The matrix $[K]_A$ contains all the orthotropic terms in $[K]$ for several axial wavelengths (mode shapes) and the anisotropic terms which

result from the combination of wavelengths. Similarly, the matrix $[B]_A$ contains all the terms found in $[B]$ for several wavelengths. There is no anisotropic contribution to $[B]_A$ because of orthogonality. Therefore, for 5 values of m , $N=5$ in equations (9) and the matrices $[K]_A$ and $[B]_A$ have dimensions 45 by 45. The eigenvalue problem whose solutions are the square of the natural vibration frequencies of an anisotropic cylinder is shown in equation (10).

$$[K]_A \begin{Bmatrix} -o \\ u_1 \\ -o \\ v_1 \\ -o \\ w_1 \\ -a \\ u_1 \\ \cdot \\ \cdot \\ \cdot \\ -a \\ w_N \\ -1 \\ u_N \\ -1 \\ v_N \\ -1 \\ w_N \end{Bmatrix} = \omega^2 [B]_A \begin{Bmatrix} -o \\ u_1 \\ -o \\ v_1 \\ -o \\ w_1 \\ -a \\ u_1 \\ \cdot \\ \cdot \\ \cdot \\ -a \\ w_N \\ -1 \\ u_N \\ -1 \\ v_N \\ -1 \\ w_N \end{Bmatrix} \quad (10)$$

The number of wavelengths which needs to be included in equations (10) to obtain accurate frequencies is dependent on the geometry and properties of the cylinder. Including an infinite number of wavelengths would give the most accurate solution. Approximate solutions are obtained by using a limited number of wavelengths. The more wavelengths used, the more accurate are the frequencies, but as each additional wavelength is added, the difference between frequencies predicted by equation (10) with N and with $N+1$ wavelengths decreases until the predicted load has converged to the

same frequency as predicted by an infinite number of wavelengths. The natural vibration frequency for an axially loaded cylinder is found in the same way as for the orthotropic cylinder.

RESULTS AND DISCUSSION

Natural vibration frequencies of laminated cylinders are determined from the conventional first-order transverse-shear deformation theory and the present higher-order transverse-shear deformation theory. The cylinders are assumed to be simply supported and without any initial geometric imperfections.

Natural Vibration Frequencies of Orthotropic Cylinders

Natural vibration frequencies predicted by the conventional first-order transverse-shear deformation theory are compared to frequencies predicted by the present higher-order theory for cylinders of laminates $[\pm 45/90]_{4s}$ and $[\pm 45]_{6s}$ in figure 1. Several radius-to-thickness ratios, R/t , and length-to-radius ratios, L/R are included for each laminate. Vibration frequencies predicted by the first-order theory are represented by the solid curves and those predicted by the higher-order theory are represented by the dashed curves. Frequencies for circumferencial wave numbers $n=1$ through 10 are presented for three cylinder geometries. The natural frequencies are expressed in terms of a nondimensional parameter, $\bar{\omega} = \omega \sqrt{\rho R^2 / E_t}$, based on the

density, ρ , and stiffness, E_t , of the material and the radius, R , and natural frequency, ω , of the cylinder.

The in-plane material properties of Hercules Incorporated AS4-3502 graphite-epoxy unidirectional preimpregnated tape are assumed for the study (i.e., $E_l/E_t = 11.3$, $G_{lt}/E_t = .53$). The transverse properties assumed for the study are based on references 10 and 11 and are $G_{lz}/G_{lt} = 1.$, $G_{tz}/E_z = 1.$ and $G_{tz}/G_{lt} = .57$, (where l , t , and z represent the longitudinal, transverse and through-the-thickness directions of a 0-degree unidirectional laminate, respectively). In laminate definitions stacking sequences are defined such that each lamina of a given cylinder is of the same thickness (i.e., $t_{ply} \neq .005$ etc.). Calculations are based on the radius, length and total thickness of each cylinder.

Including anisotropic effects in the analysis of the $[\pm 45/90]_{4s}$ and the $[\pm 45]_{6s}$ laminated cylinders has no effect on the natural vibration frequencies. These laminates are mildly anisotropic and can be considered to be orthotropic. For cylinders of both laminates and with $R/t=100$ and $L/R=10$, the first-order theory accounts for all effects of transverse shearing which are predicted by the higher-order theory. The solid and dashed curves are identical. For the cylinder geometries with $R/t=10$ and $L/R=10$ and with $R/t=5$ and $L/R=2$, the first-order theory does not account for all effects of transverse shearing which are predicted by the higher-order theory. The difference between the predictions of the two theories can be seen for the higher wave numbers. The larger the wave number, the more significant is the reduction in vibration frequency due to transverse shearing.

Natural Vibration Frequencies of Anisotropic Cylinders

Anisotropy can have a significant effect on the natural vibration frequencies of laminated cylinders. In the study of natural vibration frequencies which follows, only the effects of the material properties and cylinder geometries are examined.

Vibration frequencies for three cylinder geometries with two stacking sequences of unsymmetrically laminated cylinders, $[90/45]_T$ and $[45/90]_T$, are shown in figure 2. The results are presented for predictions based on the first-order and higher-order theories by assuming that anisotropic effects are neglected (the curves labeled "orthotropic") and by assuming that anisotropic effects are included (the curves labeled "anisotropic"). As in figure 1, the same frequencies are predicted by the first- and higher-order theories for the thin-walled cylinder, with $R/t=100$ and $L/R=10$. However, there is a reduction in the predicted frequencies due to anisotropic effects. For these laminates the effect of anisotropy on the natural vibration frequencies is more significant than the effect of transverse shear deformation. Similar effects are shown for the thicker-walled cylinders. The first- and higher-order theories predict almost the same natural vibration frequencies for low wave numbers but not for higher wave numbers. Both transverse shear deformation and anisotropic effects reduce the predicted natural vibration frequencies. The difference between the two solid lines is the difference between the orthotropic prediction and the anisotropic prediction for the first-order theory. The difference between the two dashed lines is the difference between the orthotropic prediction and the anisotropic prediction for the higher-order theory. The difference

between the higher solid and higher dashed lines is the difference between the orthotropic prediction of first- and higher-order theories. The difference between the lower solid and lower dashed lines is the difference between the anisotropic prediction of first- and higher-order theories. For each cylinder geometry the difference between the two solid lines or the two dashed lines is larger than the difference between the higher dashed and solid lines or the lower dashed and solid lines. There is little dependence of the natural frequencies on the details of ply orientation, the laminate with the 90° ply on the outside and the 45° ply on the inside of the cylinder has almost the same natural vibration frequencies as the cylinder with the plies reversed.

The natural vibration frequencies for three cylinder geometries with $[\pm 45]_s$ laminates are shown in figure 3. For the thin-walled cylinder and the moderately thick-walled cylinder, the effects of anisotropy are more significant than the effects of transverse shearing. For the thickest-walled cylinder, the effects of transverse shearing are more significant than the effects of anisotropy. For all three geometries, the effects of both anisotropy and transverse shearing become more important as the circumferential wave number increases.

Effect of Stacking Sequence on Natural Vibration Frequencies

Results of parametric studies of the effects of stacking sequence on the natural vibration frequencies for cylinders with $[\pm\theta/90]_{4s}$ and $[\pm\theta]_s$ laminates are shown in figures 4 and 5, respectively. The same nondimensional parameter used to express the natural vibration frequency in

figures 1-3 is used in figures 4 and 5. The dependence of the natural frequency on the value of θ ranging from 0° to 90° is shown for three cylinder geometries. Natural frequencies for two wave numbers, the one producing the lowest natural vibration frequency (generally $n=1$ or $n=2$) and $n=10$, are shown for the first-order and the higher-order transverse-shear deformation theories.

For the thin-walled cylinders, the effect of transverse-shear deformation is negligible for both wave numbers shown in figures 4 and 5. However, transverse shearing does decrease the natural vibration frequencies in the thicker-walled cylinders. The most significant difference in natural vibration frequency between the first-order theory and the higher-order theory is when $n=10$ and $R/t=5$. For the thick-walled cylinders vibrating at high frequencies, the additional effects of transverse shearing predicted by the higher-order theory lead to predictions of natural vibration frequencies which are 10 percent lower than predictions based on the first-order theory for both types of laminates.

The effects of anisotropy decrease natural vibration frequencies by as much as the effects of transverse shearing in strongly anisotropic laminates. Anisotropic effects are most significant for the higher frequencies with $35^\circ < \theta < 55^\circ$.

Natural Vibration Frequencies of Cylinders Subjected to Axial Compression

Natural vibration frequencies of laminated cylinders subjected to axial compressive loads are shown in figures 6-8. The solid lines represent the interaction of axial compressive loads and natural vibration frequencies

based on the first-order theory. The dashed lines represent the interaction based on the higher-order theory. The frequencies are expressed as a function of applied axial compressive load for cylinders with laminates $[\pm 45/90]_{4s}$ in figure 6 and $[\pm 45]_s$ in figure 7 for low wave numbers and with $[\pm 45/90]_{4s}$ in figure 8 for high wave numbers. The results are expressed in nondimensional parameters based on the frequency when no load is applied and the axial compressive buckling load when the cylinder is not vibrating.

The effects of transverse shearing on the natural vibration frequency are very small for low wave numbers for all three cylinders shown. The effects of transverse shearing on the axial compressive buckling load is significant in the case of the very thick-walled cylinder but not in the other cases studied. The frequencies and loads are shown for two wave numbers in figure 6.

Anisotropic effects are more significant than transverse-shearing effects for the lower vibration frequencies of the strongly anisotropic laminate, $[\pm 45]_s$, for both an applied axial compressive load and for a vibration frequency. However, the effects of anisotropy are more important in predicting the axial compressive buckling load. The difference in buckling loads predicted by including anisotropic effects and by neglecting them is about 15 percent while the difference in the lowest natural vibration frequencies predicted by including anisotropic effects and by neglecting them is only about 5 percent. The effect of accounting for transverse shearing which is neglected by the first-order theory is to reduce the buckling load by less than 5 percent and the frequency by less than 3 percent.

The interaction curves for wave number $n=10$ of two $[\pm 45/90]_{4s}$ laminated cylinders are shown in figure 8. The first cylinder is thin walled ($R/t=100$) and the second cylinder is thick walled ($R/t=10$). Almost no difference can be seen in the predictions based on the first- and higher-order theories for the thin-walled cylinder. Anisotropic effects do not affect the vibration frequency when little axial compressive load is applied, but they become important when the axial compressive load approaches the critical buckling load of the cylinder. When only axial compression is applied, neglecting anisotropic effects leads to a predicted buckling load which is about 7 percent higher than the predicted buckling load found by including anisotropic effects.

There is a significant difference between the predictions based on the first- and higher-order theories for the thick-walled cylinder. Transverse-shear deformation effects reduce the predicted natural vibration frequency by about 7 percent and the predicted buckling load by about 7 percent. Anisotropic effects do not affect the vibration frequency when little axial compressive load is applied. Neglecting them leads to a predicted buckling load which is about 4 percent higher than predicted buckling loads found by including them when only an axial compressive load is applied. The interaction curves of both cylinders have a constant frequency ratio for axial compressive loads less than 40 percent of the critical buckling load. For the higher wave number, $n=10$, the minimum eigenvalue is found when the axial wave number m is equal to one when the frequency ratio is greater than .9. The minimum eigenvalue is found at $m=1$ when the axial compression ratio is less than .3 for the thin-walled cylinders and less than .66 for the thick-walled cylinders. When the axial compression ratio

is greater than .85, the axial wave number is constant for a given cylinder. For the thin-walled cylinder that constant wave number is $m=24$. For the thick-walled cylinder it is $m=38$. The curved section of each interaction curve is the transition range when the axial compression ratio is below .85 for thin- and thick-walled cylinders and is above .3 for the thin-walled cylinders and above .66 for the thick-walled cylinders.

Natural Vibration Frequencies in Accoustic Range

Natural vibration frequencies can be of concern when evaluating noise transmission characteristics of composite plates and shells (ref. 12). The frequency range of most concern is between 100 Hz and 10 kHz. All the frequencies shown on figure 1 for the thin-walled shell ($R/t=100$) are within this frequency range except for the minimum frequency for $n=2$. The frequencies for $n=1-3$ are in the accoustic range for the thick-walled shell ($R/t=10$) but none of the frequencies shown in figure 1 are in this range for the very thick-walled shell ($R/t=5$).

In comparing graphite-epoxy and aluminum panels designed to carry the same load, the graphite-epoxy panels are usually lighter and have higher fundamental vibration frequencies. Studies (e.g., ref. 12) indicate that composite panels have higher transmission loss than aluminum panels at or below the fundamental vibration frequency of the comparable aluminum panel. For frequencies above the fundamental vibration frequency of the aluminum panel, the aluminum panels have higher transmission loss because of their higher weight. Since higher transmission loss is desirable, composite panels may be useful for suppressing low frequency noise transmission problems.

CONCLUDING REMARKS

An analytical study of the effects of transverse shear deformation and anisotropy on the natural vibration frequencies of orthotropic and anisotropic laminated cylinders was conducted. The effects on natural vibration frequencies of adding higher-order terms in the form of trigonometric terms through-the-thickness to the displacement series of conventional first-order transverse-shear deformation shell theories were studied. Natural vibration frequencies predicted by the first-order transverse-shear deformation theory and the higher-order theory were compared to determine which cylinder geometries and laminate stacking sequences have a reduction in natural vibration frequencies due to transverse shearing. A parametric study of natural vibration frequencies of cylinders with $[\pm\theta/90]_{ns}$ and $[\pm\theta]_{ns}$ laminates was conducted to determine which laminates are most sensitive to transverse-shear deformation effects. Anisotropic effects were studied by comparing natural vibration frequencies predicted by the first-order transverse-shear deformation theory and by the higher-order theory with anisotropic material properties neglected and with anisotropic material properties included. The interaction of axial compression and natural vibration frequencies was also studied. Natural vibration frequencies were evaluated for cylinders subjected to axial compressive loadings up to the critical buckling load of the cylinder with no vibration.

Transverse shear deformation and anisotropy have the largest effect on natural vibration frequencies in cylinders which are moderately-thick- (e.g., $R/t=10$) or thick-walled (e.g., $R/t=5$) and for higher vibration

frequencies. In thin-walled cylinders no effects of transverse shear deformation are predicted by the higher-order theory which are not predicted by the first-order theory. For moderately-thick- and thick-walled cylinders, the effects of transverse shear deformation on the natural vibration frequencies are significant for higher wave numbers. Anisotropy has a significant effect on higher vibration frequencies of strongly anisotropic laminated cylinders, such as those with a $[\pm 45]_s$ wall laminate.

Results of parametric studies of cylinders with $[\pm\theta/90]_{4s}$ and $[\pm\theta]_s$ laminates indicate that first-order theory is accurate at predicting natural vibration frequencies for low wave numbers for all values of θ from 0° to 90° . For higher wave numbers, the natural vibration frequencies predicted by the higher-order theory are slightly below those predicted by the first-order theory for θ near 90° but are significantly below those predicted by the first-order theory for θ near 45° for the thicker-walled cylinders. Anisotropic effects are also most significant for the higher frequencies when θ is near 45° . The anisotropic effects are negligible for all values of θ not between about 35° and 55° for both types of stacking sequences.

Transverse shearing has a significant effect on the axial compressive buckling load of thick-walled cylinders. The higher-order theory predicts buckling loads which are as low as 65% of those predicted by the first-order theory for some thick-walled cylinders. Transverse shear deformation does not affect the natural vibration frequencies as strongly as it affects the axial compressive buckling load. The natural vibration frequencies of laminated cylinders subjected to axial compressive loads indicate that the natural vibration frequency is reduced only when the compressive load

approaches the critical buckling load of the cylinder which is not vibrating. The significance of the applied compressive load on the vibration frequencies is dependent upon the laminate, the cylinder geometry and the wave number. For higher frequencies an axial compressive buckling load is not significantly affected by the applied vibration unless the frequency is within 20% of the natural frequency of the unloaded cylinder. For lower frequencies the buckling load may be affected significantly when the applied vibration is much less than 20% of the natural vibration frequency of the unloaded cylinder.

REFERENCES

1. Leissa, A. W.: Vibration of shells. NASA SP-288, 1973.
2. Greenberg, J. B.; and Stavsky, Y.: Buckling and Vibration of Orthotropic Composite Cylindrical Shells. *Acta Mechanica*, vol. 36, no. 1-2, 1980, pp. 15-29.
3. Noor, Ahmed K.; and Whitworth, Sandra L.: Model Size Reduction for Buckling and Vibration Analyses of Anisotropic Panels. *Journal of Engineering Mechanics*, vol. 113, no. 2, February 1987, pp. 170-185.
4. Bert, C. W.; Baker, J. L.; and Egle, D. M.: Free Vibrations of Multilayer Anisotropic Cylindrical Shells. *Journal of Composite Materials*, vol. 3, July 1969, pp. 480-499.
5. Dong, Stanley B.: Free Vibration of Laminated Orthotropic Cylindrical Shells. *Journal of the Acoustical Society of America*, vol. 44, no. 6 December 1968, pp. 1628-1635.
6. Stein, Manuel: "Nonlinear Theory for Laminated and Thick Plates and Shells Including the Effects of Transverse Shearing. Proceedings of the 26th AIAA/ASME/ASCE/AHS Structures, Structural Dynamics and Materials Conference, AIAA Paper No. 85-0671-CP, April 1985.
7. Stein, Manuel: Nonlinear Theory for Thick Plates and Shells Including the Effects of Transverse Shearing. *AIAA Journal*, vol. 24, no. 9, September 1986, pp. 1537-1541.
8. Jegley, Dawn C.: An Analytical Study of the Effects of Transverse Shear Deformation and Anisotropy on the Buckling of Laminated Cylinders. Masters thesis, George Washington University, September 1987. Also available as NASA TM 100508, October 1987.

9. Novozhilov, V. V.: Foundations of the Nonlinear Theory of Elasticity. Graylock Press, 1953, Rochester, New York.
10. Seide, Paul; and Chang, Peter N.-H.: Finite Element Analysis of Laminated Plates and Shells, Volume 1, Annual Progress Report. March 1977 - March 1978, NASA CR 157106.
11. Rubben, A.; and Scharr, G.: Method to Determine the Complete Three-Dimensional Elastic Compliance Matrix of Composite Materials. Composite Structures, vol. 3, 1985, pp. 760-773.
12. Roussos, Louis A.; Grosveld, Ferdinand W.; Koval, Leslie R.; and Powell: Clemans A., Noise Transmission Characteristics of Advanced Composite Structural Materials. Proceedings of the 8th AIAA Aeroacoustics Conference, AIAA Paper no. 83-0694, April 1983.

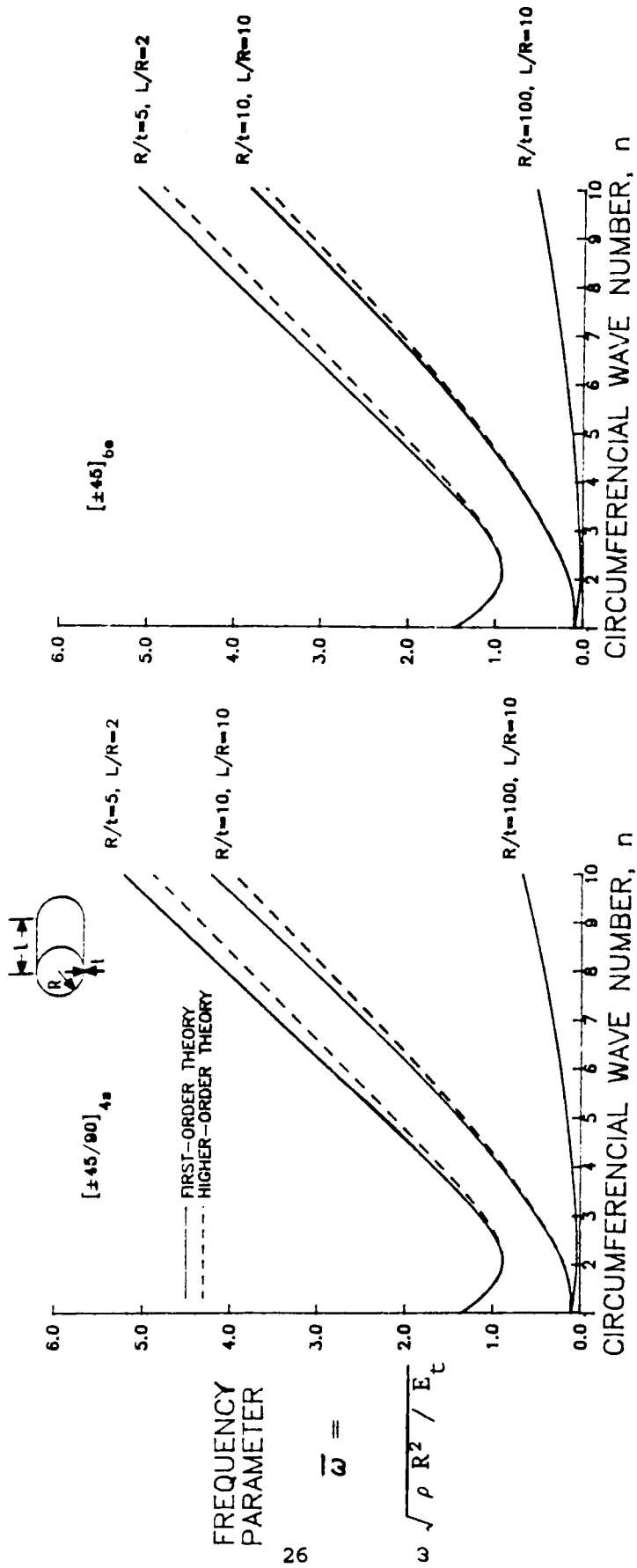
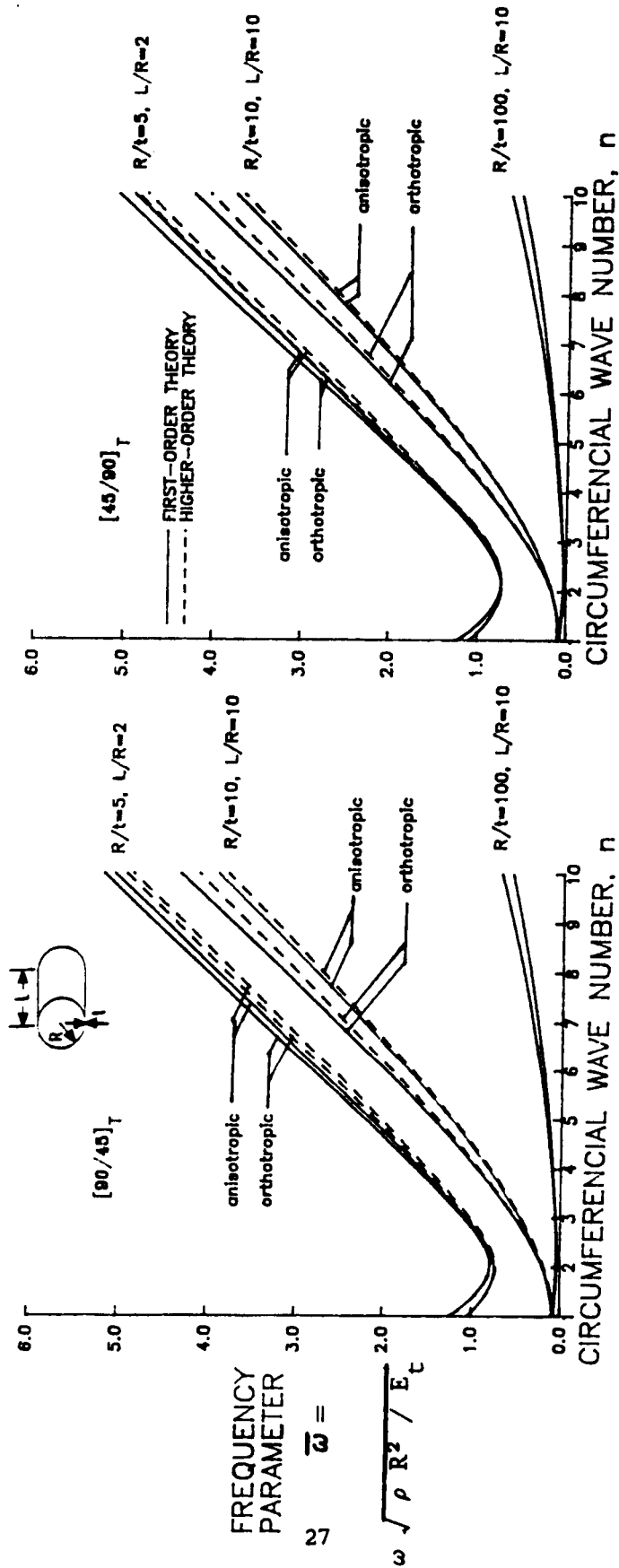


Figure 1. Effect of transverse shearing on natural vibration frequencies of orthotropic $[\pm 45/90]_{4s}$ and $[\pm 45]_{6s}$ laminated cylinders for three cylinder geometries for one to ten circumferential waves.



ORIGINAL PAGE IS
OF POOR QUALITY

Figure 2. Effect of transverse shearing and anisotropy on natural vibration frequencies of unsymmetric laminates $[45/90]_T$ and $[90/45]_T$ for three cylinder geometries for one to ten circumferential waves.

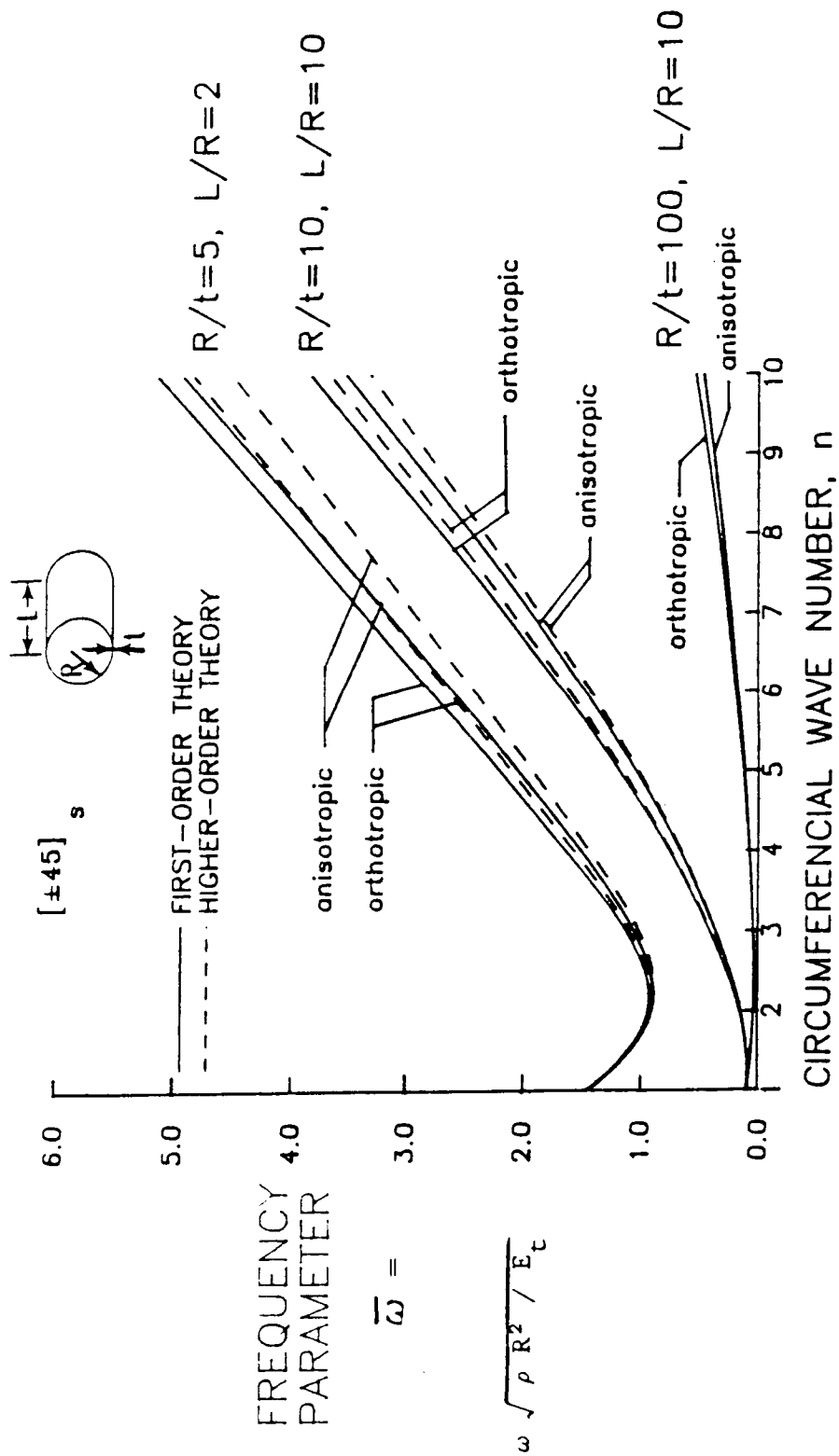


Figure 3. Effect of transverse shearing and anisotropy on natural vibration frequencies of anisotropic laminates $[\pm 45]_s$ for three cylinder geometries for one to ten circumferential waves.

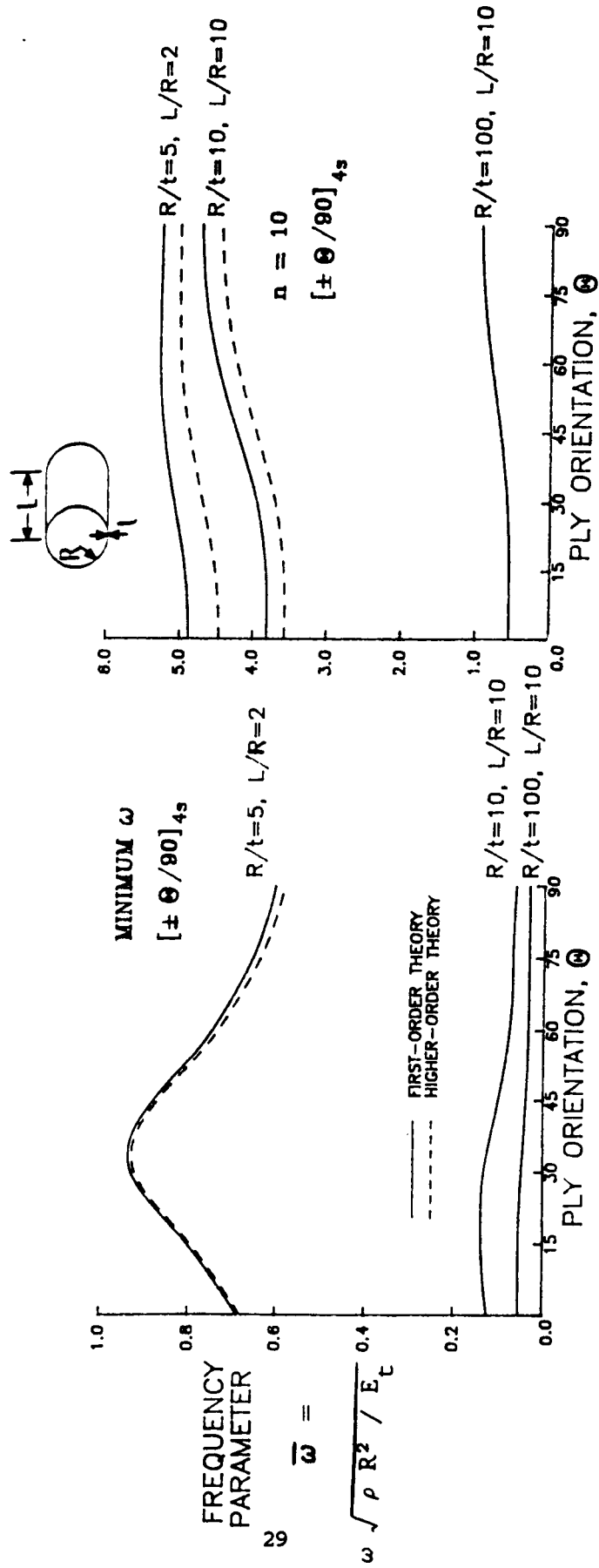


Figure 4. Effect of stacking sequence and transverse shearing on orthotropic laminates $[\pm\theta/90]_{4s}$ for $0^\circ < \theta < 90^\circ$.

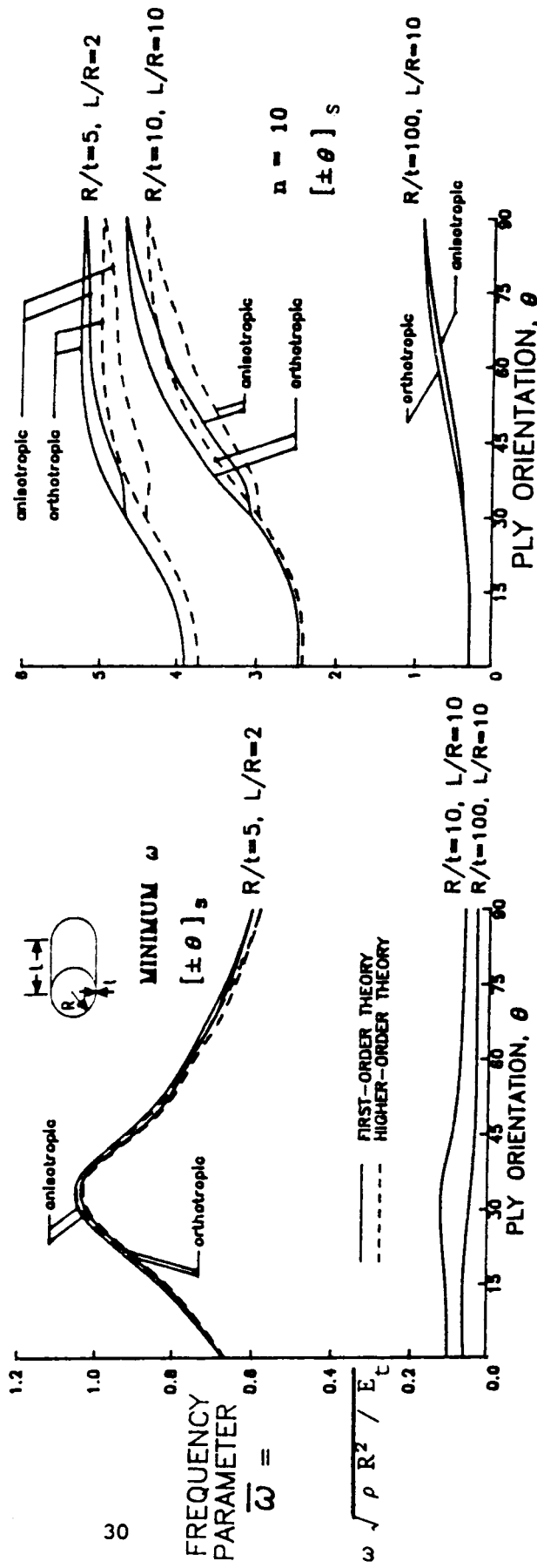


Figure 5. Effect of stacking sequence, transverse shearing and anisotropy on $[\pm\theta]_s$ laminated cylinders.

ORIGINAL PAGE IS
OF POOR QUALITY

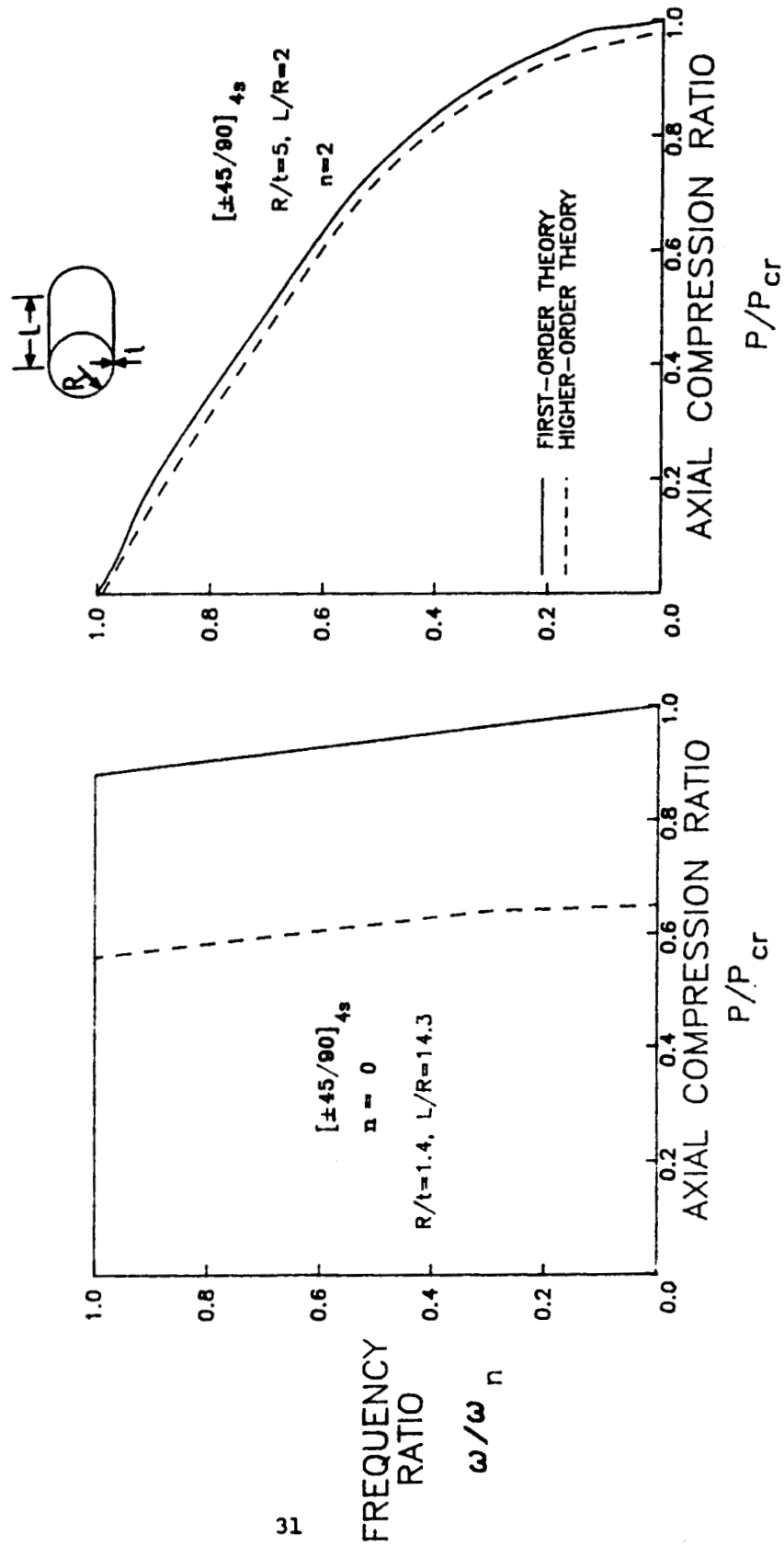


Figure 6. Interaction of axial compression and natural vibration frequency of orthotropic $[\pm 45/90]_{4s}$ laminated cylinders for low circumferential wave numbers.

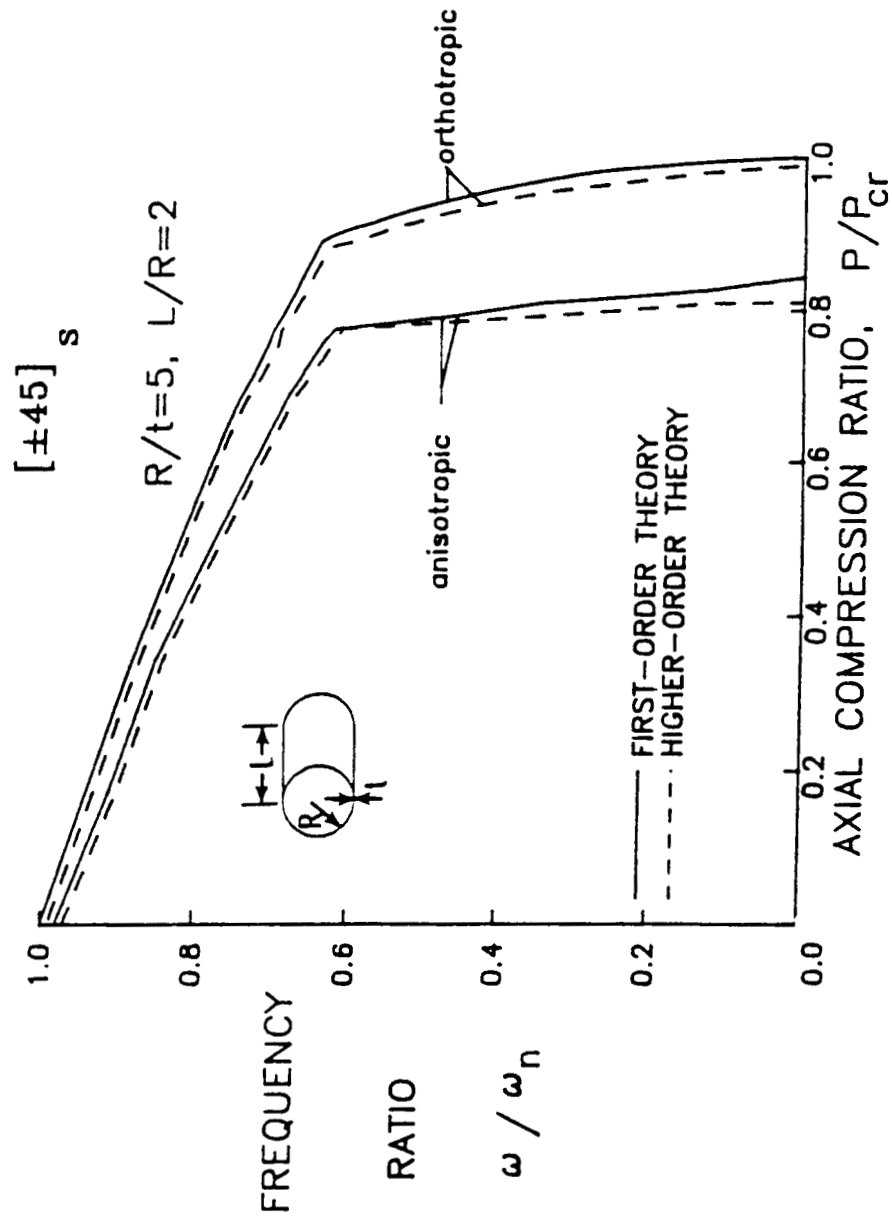


Figure 7. Interaction of axial compression and natural vibration frequency of anisotropic [±45]_s laminated cylinders.

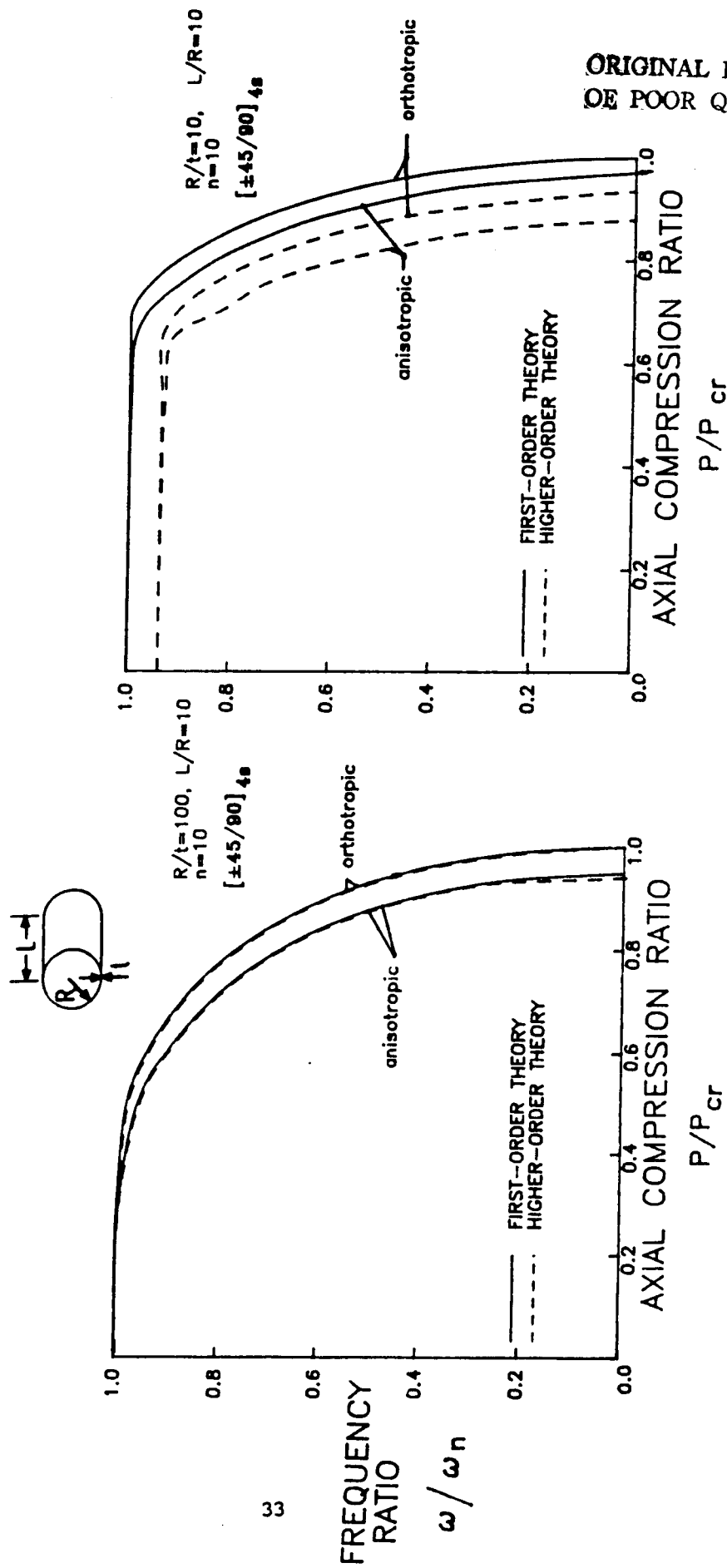


Figure 8. Interaction of axial compression and natural vibration frequency of anisotropic $[\pm 45/90]_{4s}$ laminated cylinders.



National Aeronautics and Space Administration

Report Documentation Page

1. Report No. NASA TM-100554		2. Government Accession No.		3. Recipient's Catalog No.	
4. Title and Subtitle An Analytical Study of the Effects of Transverse Shear Deformation and Anisotropy on Natural Vibration Frequencies of Laminated Cylinders				5. Report Date January 1988	
				6. Performing Organization Code	
7. Author(s) Dawn C. Jegley				8. Performing Organization Report No.	
				10. Work Unit No. 505-63-01-09	
9. Performing Organization Name and Address NASA Langley Research Center Hampton, VA 23665-5225				11. Contract or Grant No.	
				13. Type of Report and Period Covered Technical Memorandum	
12. Sponsoring Agency Name and Address National Aeronautics and Space Administration Washington, DC 20546				14. Sponsoring Agency Code	
15. Supplementary Notes					
16. Abstract Natural vibration frequencies of orthotropic and anisotropic simply supported right circular cylinders are predicted using a higher-order transverse-shear deformation theory. A comparison of natural frequencies predicted by first-order transverse-shear deformation theory and the higher-order theory shows that an additional allowance for transverse shear deformation has a negligible effect on the lowest predicted natural vibration frequencies of laminated cylinders but significantly reduces the higher natural vibration frequencies. Interaction curves for cylinders subjected to axial compressive loadings and low natural vibration frequencies indicate that transverse shearing effects are less important in predicting low natural vibration frequencies than in predicting axial compressive buckling loads. The effects of anisotropy are more important than the effects of transverse shear deformation for most strongly anisotropic laminated cylinders in predicting natural vibration frequencies. However, transverse-shear deformation effects are important in predicting high natural vibration frequencies of thick-walled laminated cylinders. Neglecting either anisotropic effects or transverse-shear deformation effects leads to non-conservative errors in predicted natural vibration frequencies.					
17. Key Words (Suggested by Author(s)) Composite Materials Transverse Shearing Anisotropy Vibration			18. Distribution Statement Unclassified - Unlimited Subject Category - 24		
19. Security Classif. (of this report) Unclassified		20. Security Classif. (of this page) Unclassified		21. No. of pages 34	22. Price A03